AIMS Mathematics, 11(3): 8521–8545.
DOI:10.3934/math.2026351
Received: 01 February 2026
Revised: 17 March 2026
Accepted: 23 March 2026
Published: 30 March 2026

https://www.aimspress.com/journal/Math

Research article

Analyzing wave dynamics with noise effects: Exploring the stochastic Zhiber–Shabat model in engineering and mathematical physics

Jan Muhammad[1], **Ali H. Tedjani**[2] **and Usman Younas**[1,*]

[1] Department of Mathematics, Shanghai University, Shanghai 200444, China

[2] Department of Mathematics and Statistics, College of Science, Imam Mohammad Ibn Saud Islamic University (IMSIU), Riyadh 11564, Saudi Arabia

* **Correspondence:** Email: usmanalgebra@shu.edu.cn.

Abstract: This paper is concerned with analytical solutions of the stochastic Zhiber–Shabat equation with a multiplicative noise term. This model is said to be an excellent tool to investigate the behavior of integrable dynamics under uncertainty. Applications exist in many areas, such as optical communications, fluid mechanics, propagation of waves through complex media, and areas that interface between mathematics, physics, and data science. We examine solitary wave solutions of the proposed model by the modified generalized exponential rational function method, generalized Arnous method, and the modified F-expansion method. The suggested methodologies suggest different soliton solutions, which are dark, bright, exponential, bright-dark, periodic, and mixed-form solutions. A range of graphs with noise term effects is used to present the behavior of the solutions with respect to the various parametric values. This paper offers a new understanding phenomenon of nonlinear waves as it measures the effectiveness of contemporary mathematical tools and explains the peculiarities of the system dynamics.

Keywords: nonlinear dynamics; noise effect; solitons; mathematical methods; stochastic Zhiber–Shabat model
Mathematics Subject Classification: 35A20, 35B10, 35C08, 60H15

1. Introduction

Nonlinear partial differential equations (NLPDEs) are very important way for modeling complex systems. Nevertheless, researchers encounter major challenges in the form of nonlinearity. Numerous researchers from various disciplines have attempted to address this difficulty by generating an extensive number of numerical and analytical approaches to find achievable solutions to nonlinear equations. Due to the high-order nature of NLPDEs, there is no universal approach. It would seem that certain

strategies may solve demanding NLPDEs with restrictions. A diversity of areas, such as engineering, biology, physics, and economics often use partial differential equations (PDEs) to govern the dynamic processes [1–3]. These equations illustrate how features such as temperature, displacement, and wave function vary over time and space. To understand how physical systems work, one must be familiar with these equations. It is typically hard to find simple analytical solutions to nonlinear equations that involve the rate of change of a variable because they are so complicated [4,5]. Such types of equations are more exact than their linear counterparts because they demonstrate how different variables are related to each other in a complicated way [6].

Solitons are of particular interest in mathematical physics, applied mathematics, and pure mathematics because they are highly stabilized and are particles in the nonlinear systems. Other areas in applied mathematics and mathematical physics can apply solitons to model phenomena. It is as such that they are critical to technology and engineering. Soliton solutions of the Zhiber–Shabat equation are particularly significant in mathematical physics because they are strongly connected to nonlinear wave events, field theory, and systems that may be integrated. These solutions are correct, stable, and limited, which make them incredibly helpful for understanding how nonlinear dynamics function in complex physical systems. The dynamics of waves are critical fields of study because waves have the ability to maintain their form and energy despite the interaction with other waves. The use of NLPDEs requires solitons because they are stable and limited wave packets that maintain their shape and speed [7]. The Schrödinger equation (NLSE) [8] and the Korteweg-de Vries (KdV) equation [9] are widely used to model different physical phenomena. The collapse of soliton-like bubbles by cavitation to launch microbots were studied in [10]. Optical soliton formation and dynamic characteristics are important phenomena which were investigated in [11]. It is much harder to understand how waves interact with each other, how energy moves, and how coherent structures change over time when these equations are nonlinear; these phenomena were studied in [12–14].

Developing exact solutions for a wide variety of physical processes allows for a more thorough understanding of physical behavior and provides a framework for further research. Exact solutions may only be obtained by expressing the dynamics of the physical system as an ordinary differential equation or a partial differntial equation. The mathematical representation of complex natural and industrial processes can only be achieved via the use of NLPDEs. Many researchers have come up with different ways to deal with these problems. Throughout the years, various techniques have been widely used, such as a variety of soliton solutions to the generalized Kadomtsev–Petviashvili equation by the application of the generalized unified method [15]. Moreover, the Kumar–Malik method and the polynomial expansion method were applied to study the the Biswas–Arshed equation, a key mathematical model describing soliton propagation in optical fibers [16, 17], and modified auxiliary equation method as well as the generalized projective Riccati equation method have been under consideration for the nonlinear generalized geophysical KdV equation in shallow water waves [18]. The nonlinear fractional Westervelt model in ultrasound imaging was explored by the improved generalized exponential rational function technique [19], and the symmetry analysis was applied to find the exact solutions of the seventh-order time fractional Sawada–Kotera–Itô equation [20]. In addition, more detail of various analytical methods can be found in [21–26]. Symmetry and antisymmetry properties of solitons governed by various NLPDEs were detailed in [27,28]. Further, the dark solitons of nonlinear lattices were studied in [29, 30]. More detail about solitons can be found in [31–33], and a detailed study of stochastic analysis can be found in [34–36].

The novelty of this work lies in the analysis of soliton dynamics in the stochastic Zhiber–Shabat equation with a Brownian motion term, using new and advanced analytical techniques. Advanced integration techniques are used to get diverse soliton solutions, including the modified generalized exponential rational function method (mGERFM) [37], the generalized Arnous method [38], and the modified F-expansion method [39]. These are effective analysis tools that help to establish precise solutions of v arious NLPDEs. The process of mGERFM is to assume a solution to be a rational expression of exponential and then to systematically find the parameters to represent solitons, periodic waves, or rational solutions. The generalized Arnous method, on the other hand, builds solutions using a balance between nonlinear and derivative terms and expresses the solution in a well-defined functional form, in which explicit traveling wave solutions are possible. At the same time, the F-expansion technique forms solutions in the form of an auxiliary function that fulfills a simple differential equation, which subsequently produces several forms of wave structures, including solitons, periodic, and hyperbolic solutions. Collectively, these techniques give flexible means of dynamically studying nonlinear systems. The results obtained indicate the flexibility and applicability of these methodologies, indicating that they are practical tools that have strong applications to the engineering and science fields. These approaches do not ignore the considerable findings that can evolve a variety of scientific fields and generate new solitons and waveforms.

Furthermore, in the case of the stochastic Zhiber–Shabat equation, the applied analytical tools have both advantages and limitations. The mGERFM is beneficial, as it is able to generate a large number of explicit wave solutions, both solitary and periodic, and its rational exponential form allows nonlinear wave dynamics to be represented flexibly. The downside, however, is that in this method, the necessary parameters and balancing conditions must be carefully chosen, and the resultant algebraic system may turn out to be complex, particularly when there are stochastic terms involved. The generalized Arnous approach is useful to build traveling wave solutions and often results in relatively simple forms of analysis, so can be used to understand qualitative effects of the stochastic Zhiber–Shabat equation; however, it can produce only a relatively small set of solutions, and can be inadequate in capturing all stochastic effects. The modified F-expansion technique is rather easy to use, and it can generate hyperbolic, trigonometric, and rational wave solutions, which is useful in the analysis of various wave structures. Its limitation is that the assumed auxiliary function restricts the possible forms of solutions, and therefore, some complex stochastic behaviors of the equation may not be fully described by this approach.

The article is arranged as follows: The governing equation is presented in Section 2, and methods are applied in Section 3. Section 4 provides discussion of the method's results and the conclusion is presented in Section 5.

2. The studied model

The investigation of soliton solutions to the nonlinear Zhiber–Shabat equation is of considerable interest and has numerous applications across various scientific domains, including nonlinear optics, solid-state physics, fluid dynamics, plasma physics, mathematical biology, dislocations in crystals, chemical kinetics, kink dynamics, and quantum field theory. The stochastic generalization of the Zhiber–Shabat equation, with a multiplicative noise term [40] reads as:

$$V_{xt} + \alpha e^{V} + \beta e^{-V} + \eta e^{-2V} = \gamma V_x \kappa_t, \tag{2.1}$$

where $V = V(x,t)$ is an unknown function, and the parameters α, β, and η are real-valued constant parameters appearing in the nonlinear terms of the model, and γ is a controlling term for the Brownian motion with $\kappa_t = \frac{d\kappa(t)}{dt}$. The noise term introduces random fluctuations that cause the wave amplitude and shape to vary over time, especially in regions with steep gradients. As a result, solitons or traveling waves can shift position, distort, or even fluctuate unpredictably, with stronger noise leading to more pronounced effects. The Wiener process is a core continuous-time stochastic process in mathematics, named after Norbert Wiener for his work on the mathematical properties of Brownian motion (a phenomenon first noted by Robert Brown). Characterized by stationary independent increments, it is one of the best-known stochastic processes and finds extensive use in fields including pure and applied mathematics, economics, physics, and evolutionary biology. Crucially, in pure mathematics, the Wiener process facilitates the study of continuous-time martingales and provides the essential building block for defining more intricate stochastic processes. Eq (2.1) modifies into the sinh-Gordon equation when $\eta = 0$, and it changes into the Liouville equation when $\beta = \eta = 0$. Similarly, for $\beta = 0$, Eq (2.1) transforms to the Dodd-Bullough-Mikhailov equation, and for $\alpha = 0$, $\beta = -1$, $\eta = 1$ it converts to the form of Tzitzeica-Dodd-Bullough equation.

Furthermore, the model without q stochastic term was discussed in the literature using various approaches. In [41], multiple solitary wave solutions were derived using the tanh approach, and [42] obtained a variety of novel exact solutions using the $\left(\frac{1}{G'}\right)$-expansion method as well as the $\left(\frac{G'}{G}\right)$ and $\left(\frac{1}{G}\right)$ methods. In [43], soliton solutions were calculated by the use of the ansatz technique. Moreover, in [44], the proposed model investigated with the application of unified method. Similarly, stochastic phenomena in other related models have been investigated in [45,46]. This research examines the exact solutions of the proposed model using the recommended methodologies.

3. Application of the methods and soliton solutions

Consider

$$V(x,t) = \Phi(\zeta)e^{\gamma\kappa(t)-\frac{\gamma^2 t}{2}}, \quad \text{where,} \quad \zeta = x - ct, \tag{3.1}$$

where c is the wave speed. On solving the Eqs (2.1) and (3.1), we obtain

$$\alpha e^{\Phi} + \beta e^{-\Phi} + \eta e^{-2\Phi} - c\Phi'' = 0. \tag{3.2}$$

We further take

$$v = e^{\Phi} \quad \text{or } \Phi = \ln v. \tag{3.3}$$

Manipulating Eq (3.3) in Eq (3.2), we get

$$-c\left((v')^2 - vv''\right) + \alpha v^3 + \beta v + \eta = 0. \tag{3.4}$$

Now, applying the homogeneous balance principle between the terms v^3 and vv'' in Eq (3.4) gives, $N = 2$.

3.1. Modified generalized exponential rational function method

The general mGERFM [37] solution is described by

$$\Phi(\zeta) = \sigma_0 + \sum_{j=1}^{N} \sigma_j \left(\frac{\Omega'(\zeta)}{\Omega(\zeta)}\right)^j + \sum_{j=1}^{N} \nu_j \left(\frac{\Omega'(\zeta)}{\Omega(\zeta)}\right)^{-j}, \tag{3.5}$$

where

$$\Omega(\zeta) = \frac{p_1 e^{q_1\zeta} + p_2 e^{q_2\zeta}}{p_3 e^{q_3\zeta} + p_4 e^{q_4\zeta}}. \tag{3.6}$$

For $N = 2$, Eq (3.5) is written as:

$$\Phi(\zeta) = \sigma_0 + \sigma_1 \frac{\Omega'(\zeta)}{\Omega(\zeta)} + \nu_1 \left(\frac{\Omega'(\zeta)}{\Omega(\zeta)}\right)^{-1} + \sigma_2 \left(\frac{\Omega'(\zeta)}{\Omega(\zeta)}\right)^2 + \nu_2 \left(\frac{\Omega'(\zeta)}{\Omega(\zeta)}\right)^{-2}. \tag{3.7}$$

• Taking $p_i = [2, 0, 1, 1]$ and $q_i = [-2, 0, 1, -1](i = 1, 2, 3, 4)$ in Eq (3.6) offers $\Omega(\zeta) = e^{-2\zeta}\text{sech}(\zeta)$. Solving Eqs (3.7) and (3.4) provide $\sigma_1 = 4\sigma_2$, $\nu_2 = 0$, $\nu_1 = 0$, $c = \frac{\alpha\sigma_2}{2}$, $\eta = 2\alpha\left(\sigma_0 - 4\sigma_2\right)\left(\sigma_0 - 3\sigma_2\right)^2$, $\beta = -\alpha\left(3\sigma_0 - 11\sigma_2\right)\left(\sigma_0 - 3\sigma_2\right)$, and $\sigma_1 = 0$, $\sigma_2 = 0$, $\nu_1 = \frac{4\nu_2}{3}$, $c = \frac{\alpha\nu_2}{18}$, $\eta = \frac{1}{81}(-2)\alpha\left(4\nu_2 - 9\sigma_0\right)\left(\nu_2 - 3\sigma_0\right)^2$, $\beta = -\frac{1}{27}\alpha\left(11\nu_2 - 27\sigma_0\right)\left(\nu_2 - 3\sigma_0\right)$.
The combined soliton solutions can be expressed as follows

$$V_{1,1}(x,t) = e^{\gamma\kappa(t) - \frac{\gamma^2}{2}t}\left(\log\left(\frac{1}{2}\left(\sigma_0\left(\cosh\left(2x - \alpha\sigma_2 t\right) + 1\right) - \sigma_2\left(3\cosh\left(2x - \alpha\sigma_2 t\right) + 5\right)\right)\text{sech}^2\left(x - \frac{1}{2}\alpha\sigma_2 t\right)\right)\right), \tag{3.8}$$

$$V_{1,2}(x,t) = e^{\gamma\kappa(t) - \frac{\gamma^2}{2}t}\left(\log\left(\sigma_0 - \frac{\nu_2\left(4\sinh\left(2x - \frac{1}{9}\alpha\nu_2 t\right) + 5\cosh\left(2x - \frac{1}{9}\alpha\nu_2 t\right) + 5\right)}{6\left(\sinh\left(x - \frac{1}{18}\alpha\nu_2 t\right) + 2\cosh\left(x - \frac{1}{18}\alpha\nu_2 t\right)\right)^2}\right)\right). \tag{3.9}$$

• By taking $p_i = [1, 1, 1, 0]$ and $q_i = [3, 2, 0, 0](i = 1, 2, 3, 4)$, Eq (3.6) offers $\Omega(\zeta) = e^{2\zeta} + e^{3\zeta}$, and Eqs (3.7) and (3.4) give $\sigma_1 = -5\sigma_2$, $\nu_2 = 0$, $\nu_1 = 0$, $c = \frac{\alpha\sigma_2}{2}$, $\eta = \frac{1}{2}\alpha\left(4\sigma_0 - 25\sigma_2\right)\left(\sigma_0 - 6\sigma_2\right)^2$, $\beta = -\frac{1}{2}\alpha\left(6\sigma_0 - 37\sigma_2\right)\left(\sigma_0 - 6\sigma_2\right)$ so that we get

$$V_{1,3}(x,t) = e^{\gamma\kappa(t) - \frac{\gamma^2}{2}t}\left(\log\left(\sigma_0 - \frac{\sigma_2\left(6e^{\alpha\sigma_2 t} + 13e^{\frac{1}{2}\alpha\sigma_2 t + x} + 6e^{2x}\right)}{\left(e^{\frac{1}{2}\alpha\sigma_2 t} + e^x\right)^2}\right)\right). \tag{3.10}$$

Next, the hyperbolic solution is as follows

$$V_{1,4}(x,t) = e^{\gamma\kappa(t) - \frac{\gamma^2}{2}t}\left(\log\left(\frac{1}{4}\text{sech}^2\left(\frac{1}{2}(x - ct)\right)(2\sigma_0(\cosh(ct - x) + 1) - \sigma_2(12\cosh(ct - x) + 13))\right)\right). \tag{3.11}$$

Similarly, for $\sigma_1 = 0$, $\sigma_2 = 0$, $\nu_1 = -\frac{1}{6}\left(5\nu_2\right)$, $c = \frac{\alpha\nu_2}{72}$, $\eta = -\frac{\alpha(25\nu_2 - 144\sigma_0)(\nu_2 - 6\sigma_0)^2}{2592}$, $\beta = -\frac{1}{432}\alpha\left(37\nu_2 - 216\sigma_0\right)\left(\nu_2 - 6\sigma_0\right)$, we have

$$V_{1,5}(x,t) = e^{\gamma\kappa(t) - \frac{\gamma^2}{2}t}\left(\log\left(\sigma_0 - \frac{\nu_2\left(4e^{\frac{1}{36}\alpha\nu_2 t} + 13e^{\frac{1}{72}\alpha\nu_2 t + x} + 9e^{2x}\right)}{6\left(2e^{\frac{1}{72}\alpha\nu_2 t} + 3e^x\right)^2}\right)\right). \tag{3.12}$$

Next, we get

$$V_{1,6}(x,t)=e^{\gamma\kappa(t)-\frac{\gamma^2}{2}t}\left(\log\left(\frac{\nu_2(5\sinh(ct-x)-13\cosh(ct-x)-13)+6\sigma_0(-5\sinh(ct-x)+13\cosh(ct-x)+12)}{6\left(\sinh\left(\frac{1}{2}(x-ct)\right)+5\cosh\left(\frac{1}{2}(x-ct)\right)\right)^2}\right)\right). \tag{3.13}$$

• Choosing $p_i=[1,1,2,0]$ and $q_i=[i,-i,0,0](i=1,2,3,4)$, Eq (3.6) gives $\Omega(\zeta)=\cos\zeta$, and Eqs (3.7) and (3.4) provide $\sigma_1=0,\ \sigma_2=0,\ \nu_1=0,\ c=\frac{\alpha\nu_2}{2},\ \eta=2\alpha\sigma_0\left(\nu_2-\sigma_0\right)^2,\ \beta=-\alpha\left(\nu_2-3\sigma_0\right)\left(\nu_2-\sigma_0\right)$, along with $\sigma_1=0,\ \sigma_2=\nu_2,\ \nu_1=0,\ c=\frac{\alpha\nu_2}{2},\ \eta=2\alpha\left(\sigma_0-2\nu_2\right)^2\left(2\nu_2+\sigma_0\right),\ \beta=\alpha\left(2\nu_2-\sigma_0\right)\left(2\nu_2+3\sigma_0\right)$. We get the explicit periodic wave solutions:

$$V_{1,7}(x,t)=e^{\gamma\kappa(t)-\frac{\gamma^2}{2}t}\left(\log\left(\sigma_0+\nu_2\cot^2\left(x-\frac{1}{2}\alpha\nu_2t\right)\right)\right), \tag{3.14}$$

$$V_{1,8}(x,t)=e^{\gamma\kappa(t)-\frac{\gamma^2}{2}t}\left(\log\left(\sigma_0+\nu_2\left(\tan^2\left(x-\frac{1}{2}\alpha\nu_2t\right)+\cot^2\left(x-\frac{1}{2}\alpha\nu_2t\right)\right)\right)\right). \tag{3.15}$$

• Taking $p_i=[-i,-i,-i,-i]$ and $q_i=[1,-1,0,0](i=1,2,3,4)$, Eq (3.6), gives $\Omega(\zeta)=\cosh\zeta$. Equations (3.7) and (3.4) provide $\sigma_1=0,\ {}_2=0,\ \nu_1=0,\ c=\frac{\alpha\nu_2}{2},\ \eta=2\alpha\sigma_0\left(\nu_2+\sigma_0\right)^2,\ \beta=-\alpha\left(\nu_2+\sigma_0\right)\left(\nu_2+3\sigma_0\right)$, and $\sigma_1=0,\ \sigma_2=\nu_2,\ \nu_1=0,\ c=\frac{\alpha\nu_2}{2},\ \eta=-2\alpha\left(2\nu_2-\sigma_0\right)\left(2\nu_2+\sigma_0\right)^2,\ \beta=\alpha\left(2\nu_2-3\sigma_0\right)\left(2\nu_2+\sigma_0\right)$. We get the singular and dark-singular soliton solutions, respectively:

$$V_{1,9}(x,t)=e^{\gamma\kappa(t)-\frac{\gamma^2}{2}t}\left(\log\left(\sigma_0+\nu_2\coth^2\left(x-\frac{1}{2}\alpha\nu_2t\right)\right)\right), \tag{3.16}$$

$$V_{1,10}(x,t)=e^{\gamma\kappa(t)-\frac{\gamma^2}{2}t}\left(\log\left(\sigma_0+\nu_2\left(\tanh^2\left(x-\frac{1}{2}\alpha\nu_2t\right)+\coth^2\left(x-\frac{1}{2}\alpha\nu_2t\right)\right)\right)\right). \tag{3.17}$$

• Choosing $p_i=[1,-1,2,0]$ and $q_i=[2,0,0,0](i=1,2,3,4)$, Eq (3.6) gives $\Omega(\zeta)=\sinh\zeta$. Equations (3.7) and (3.4) provide $\sigma_2=-\frac{\sigma_1}{2},\ \nu_2=0,\ \nu_1=0,\ c=-\frac{1}{4}\left(\alpha\sigma_1\right),\ \eta=\alpha\sigma_0^2\left(2\sigma_0+\sigma_1\right),\ \beta=-\alpha\sigma_0\left(3\sigma_0+\sigma_1\right)$. We get solitary wave solution:

$$V_{1,11}(x,t)=e^{-\frac{1}{2}\gamma t(\gamma-2\kappa)}\log\left(\sigma_0-\frac{1}{2}\sigma_1\mathrm{csch}^2\left(\frac{1}{4}\alpha\sigma_1t+x\right)\right). \tag{3.18}$$

3.2. Generalized Arnous method

This method [38] offers the solution as:

$$\Phi(\zeta)=\sigma_0+\sum_{r=1}^{N}\frac{\sigma_r}{(\Theta(\zeta))^r}+\sum_{r=1}^{N}\frac{\nu_r\left(\Theta'(\zeta)\right)^r}{(\Theta(\zeta))^r}; \tag{3.19}$$

with $N=2$, Eq (3.19) can be written as

$$\Phi(\zeta)=\sigma_0+\frac{\sigma_1}{\Theta(\zeta)}+\frac{\nu_1\Theta'(\zeta)}{\Theta(\zeta)}+\frac{\sigma_2}{(\Theta(\zeta))^2}+\nu_2\left(\frac{\Theta(\zeta)}{\Theta(\zeta)}\right)^2, \tag{3.20}$$

and

$$(\Theta'(\zeta))^2 = \ln(\delta)^2\left(\Theta(\zeta)^2 - \rho\right), \tag{3.21}$$

with

$$\Theta^{(N)}(\zeta) = \begin{cases} \Theta'(\zeta)\ln(\delta)^{(N-2)}, & N \text{ is odd}, \\ \Theta(\zeta)\ln(\delta)^N, & N \text{ is even}, \end{cases}$$

for $\delta \neq 1$, $N \geq 2$, and $\delta > 0$. The solution to Eq (3.21) is as follows:

$$\Theta(\zeta) = A\ln(\delta)\delta^{\zeta} + \frac{\rho}{4A\ln(\delta)\delta^{\zeta}}, \tag{3.22}$$

where ρ and A are arbitrarily chosen parameters. When Eq (3.20) is combined with Eq (3.21) in Eq (3.4), the general solutions are as follows:

When $\sigma_1 = 0$, $\nu_1 = 0$, $c = \frac{1}{2}\alpha\left(\nu_2 - \frac{\sigma_2}{\rho\log^2(\delta)}\right)$, $\beta = -\frac{\alpha\left(\nu_2\log^2(\delta)+\sigma_0\right)\left(\nu_2\rho\log^2(\delta)+3\rho\sigma_0+2\sigma_2\right)}{\rho}$, $\eta = \frac{2\alpha(\rho\sigma_0+\sigma_2)\left(\nu_2\log^2(\delta)+\sigma_0\right)^2}{\rho}$.

Then, we get

$$V_{2,1}(x,t) = e^{\gamma\kappa(t)-\frac{\gamma^2}{2}t}\left(\log\left(\frac{\nu_2\left(A\log^2(\delta)\delta^{x-\frac{1}{2}\alpha t\left(\nu_2-\frac{\sigma_2}{\rho\log^2(\delta)}\right)} - \frac{\rho\delta^{\frac{1}{2}\alpha t\left(\nu_2-\frac{\sigma_2}{\rho\log^2(\delta)}\right)-x}}{4A}\right)^2}{\left(\frac{\rho\delta^{\frac{1}{2}\alpha t\left(\nu_2-\frac{\sigma_2}{\rho\log^2(\delta)}\right)-x}}{4A\log(\delta)} + A\log(\delta)\delta^{x-\frac{1}{2}\alpha t\left(\nu_2-\frac{\sigma_2}{\rho\log^2(\delta)}\right)}\right)^2} + \frac{\sigma_2}{\left(\frac{\rho\delta^{\frac{1}{2}\alpha t\left(\nu_2-\frac{\sigma_2}{\rho\log^2(\delta)}\right)-x}}{4A\log(\delta)} + A\log(\delta)\delta^{x-\frac{1}{2}\alpha t\left(\nu_2-\frac{\sigma_2}{\rho\log^2(\delta)}\right)}\right)^2} + \sigma_0\right)\right). \tag{3.23}$$

Choosing $\delta = e$ and $\rho = 4A^2$ in the solution (3.23) offers a bright-dark soliton solution:

$$V_{2,2}(x,t) = e^{\gamma\kappa(t)-\frac{\gamma^2}{2}t}\left(\log\left(\frac{\sigma_2\mathrm{sech}^2(ct-x)}{4A^2} + \nu_2\tanh^2(ct-x) + \sigma_0\right)\right). \tag{3.24}$$

Also, for $\delta = e$ and $\rho = -4A^2$, the solution (3.23) can be written as a singular soliton solution:

$$V_{2,3}(x,t) = e^{\gamma\kappa(t)-\frac{\gamma^2}{2}t}\left(\log\left(\frac{\sigma_2\mathrm{csch}^2(ct-x)}{4A^2} + \nu_2\coth^2(ct-x) + \sigma_0\right)\right). \tag{3.25}$$

Similarly, when $\sigma_1 = 0$, $\sigma_2 = \frac{\rho\log^2(\delta)(\alpha\nu_2-2c)}{\alpha}$, $\nu_1 = 0$, $\beta = -\left(\left(\nu_2\log^2(\delta)+\sigma_0\right)\left(3\alpha\nu_2\log^2(\delta)+3\alpha\sigma_0-4c\log^2(\delta)\right)\right)$, $\eta = 2\left(\nu_2\log^2(\delta)+\sigma_0\right)^2\left(\alpha\nu_2\log^2(\delta)+\alpha\sigma_0-2c\log^2(\delta)\right)$,
then we get:

$$V_{2,4}(x,t) = e^{\gamma\kappa(t)-\frac{\gamma^2}{2}t}$$

$$\left(\log\left(\frac{\alpha\nu_2\left(4A^2\log^3(\delta)\delta^{2x}+\rho\log(\delta)\delta^{2ct}\right)^2+\alpha\sigma_0\left(4A^2\log^2(\delta)\delta^{2x}+\rho\delta^{2ct}\right)^2-32A^2c\rho\log^4(\delta)\delta^{2(ct+x)}}{\alpha\left(4A^2\log^2(\delta)\delta^{2x}+\rho\delta^{2ct}\right)^2}\right)\right). \tag{3.26}$$

Setting $\delta = e$ and $\rho = 4A^2$ in the solution (3.26) provides a bright soliton solution:

$$V_{2,5}(x,t) = e^{\gamma\kappa(t)-\frac{\gamma^2}{2}t}\left(\log\left(-\frac{2c\,\mathrm{sech}^2(ct-x)}{\alpha}+\nu_2+\sigma_0\right)\right). \tag{3.27}$$

Also, with $\delta = e$ and $\rho = -4A^2$, the solution (3.26) can be expressed

$$V_{2,6}(x,t) = e^{\gamma\kappa(t)-\frac{\gamma^2}{2}t}\left(\log\left(\frac{2c\,\mathrm{csch}^2(ct-x)}{\alpha}+\nu_2+\sigma_0\right)\right). \tag{3.28}$$

3.3. Modified F-expansion method

By applying the modified F-expansion method [39], the solution for $N = 2$ can be expressed as follows:

$$\Phi(\zeta) = \sigma_0 + \sigma_1\Omega(\zeta) + \frac{\nu_1}{\Omega(\zeta)} + \sigma_2\left(\Omega(\zeta)\right)^2 + \frac{\nu_2}{\left(\Omega(\zeta)\right)^2}, \tag{3.29}$$

with

$$\Omega'(\zeta) = \hbar_2\Omega(\zeta)^2 + \hbar_1\Omega(\zeta) + \hbar_0. \tag{3.30}$$

By manipulating Eqs (3.29), (3.30), and (3.4), we get the following

• $\hbar_0 \to 0$, $\hbar_1 \to 1$, $\hbar_2 \to -1$ offers $\sigma_2 = -\sigma_1$, $\nu_1 = 0$, $\nu_2 = 0$, $\alpha = \frac{2\eta}{\sigma_0^2(4\sigma_0+\sigma_1)}$, $\beta = \frac{1}{2}\left(-\frac{12\eta}{4\sigma_0+\sigma_1} - \frac{2\eta\sigma_1}{\sigma_0(4\sigma_0+\sigma_1)}\right)$, $c = -\frac{\eta\sigma_1}{\sigma_0^2(4\sigma_0+\sigma_1)}$. The dark soliton is

$$V_{3,1}(x,t) = e^{\gamma\kappa(t)-\frac{\gamma^2}{2}t}$$
$$\left(\log\left(\sigma_0 - \sigma_1\left(\frac{1}{2}\tanh\left(\frac{1}{2}\left(\frac{\eta\sigma_1 t}{\sigma_0^2\left(4\sigma_0+\sigma_1\right)}+x\right)\right)+\frac{1}{2}\right)^2+\sigma_1\left(\frac{1}{2}\tanh\left(\frac{1}{2}\left(\frac{\eta\sigma_1 t}{\sigma_0^2\left(4\sigma_0+\sigma_1\right)}+x\right)\right)+\frac{1}{2}\right)\right)\right). \tag{3.31}$$

• $\hbar_0 \to 0$, $\hbar_1 \to -1$, $\hbar_2 \to 1$, offers $\sigma_1 = -\frac{2c}{\alpha}$, $\sigma_2 = \frac{2c}{\alpha}$, $\nu_2 = 0$, $\eta = 2\alpha\sigma_0^3 - c\sigma_0^2$, $\nu_1 = 0$, $\beta = \sigma_0\left(c - 3\alpha\sigma_0\right)$. As a result, we get

$$V_{3,2}(x,t) = e^{\gamma\kappa(t)-\frac{\gamma^2}{2}t}\left(\log\left(\frac{2c\left(\frac{1}{2}-\frac{1}{2}\coth\left(\frac{1}{2}(x-ct)\right)\right)^2}{\alpha}-\frac{2c\left(\frac{1}{2}-\frac{1}{2}\coth\left(\frac{1}{2}(x-ct)\right)\right)}{\alpha}+\sigma_0\right)\right). \tag{3.32}$$

• $\hbar_0 \to \frac{1}{2}$, $\hbar_1 \to 0$, $\hbar_2 \to -\frac{1}{2}$ offers $\sigma_1 = 0$, $\sigma_2 = 0$, $\nu_2 = \frac{c}{2\alpha}$, $\eta = \frac{\sigma_0(2\alpha\sigma_0+c)^2}{2\alpha}$, $\nu_1 = 0$, $\beta = \frac{-12\alpha^2\sigma_0^2-c^2-8\alpha c\sigma_0}{4\alpha}$ along with $\sigma_1 = 0$, $\sigma_2 = \frac{c}{2\alpha}$, $\nu_2 = 0$, $\eta = \frac{\sigma_0(2\alpha\sigma_0+c)^2}{2\alpha}$, $\nu_1 = 0$, $\beta = \frac{-12\alpha^2\sigma_0^2-c^2-8\alpha c\sigma_0}{4\alpha}$, and $\sigma_1 = 0$, $\sigma_2 = \frac{c}{2\alpha}$, $\nu_2 = \frac{c}{2\alpha}$, $\eta = \frac{2(\alpha\sigma_0-c)(\alpha\sigma_0+c)^2}{\alpha^2}$, $\nu_1 = 0$, $\beta = \frac{-3\alpha^2\sigma_0^2+c^2-2\alpha c\sigma_0}{\alpha}$. Hence, we secure
The complex bright-dark soliton solution:

$$V_{3,3}(x,t) = e^{\gamma\kappa(t)-\frac{\gamma^2}{2}t}\left(\log\left(\sigma_0+\frac{c}{2\alpha(i\,\mathrm{sech}(ct-x)-\tanh(ct-x))^2}\right)\right). \tag{3.33}$$

The combined singular soliton solution is as follows

$$V_{3,4}(x,t) = e^{\gamma\kappa(t)-\frac{\gamma^2}{2}t}\left(\log\left(\frac{c(-\coth(ct-x)-\operatorname{csch}(ct-x))^2}{2\alpha}+\sigma_0\right)\right). \tag{3.34}$$

The combined soliton solution can then be expressed as follows

$$V_{3,5}(x,t) = e^{\gamma\kappa(t)-\frac{\gamma^2}{2}t}\left(\log\left(-\frac{c(\operatorname{sech}(ct-x)-i\tanh(ct-x))^2}{2\alpha}-\frac{c}{2\alpha(\operatorname{sech}(ct-x)-i\tanh(ct-x))^2}+\sigma_0\right)\right). \tag{3.35}$$

• $\hbar_0 \to 1$, $\hbar_1 \to 0$, $\hbar_2 \to -1$ gives $\sigma_1 = 0$, $\sigma_2 = 0$, $\nu_2 = \frac{2c}{\alpha}$, $\eta = \frac{2\sigma_0(\alpha\sigma_0+2c)^2}{\alpha}$, $\nu_1 = 0$, and $\beta = \frac{-3\alpha^2\sigma_0^2-4c^2-8\alpha c\sigma_0}{\alpha}$ along with $\sigma_1 = 0$, $\sigma_2 = \frac{2c}{\alpha}$, $\nu_2 = 0$, $\eta = \frac{2\sigma_0(\alpha\sigma_0+2c)^2}{\alpha}$, $\nu_1 = 0$, $\beta = \frac{-3\alpha^2\sigma_0^2-4c^2-8\alpha c\sigma_0}{\alpha}$, and $\sigma_1 = 0$, $\sigma_2 = \frac{2c}{\alpha}$, $\nu_2 = \frac{2c}{\alpha}$, $\eta = \frac{2(\alpha\sigma_0-4c)(\alpha\sigma_0+4c)^2}{\alpha^2}$, $\nu_1 = 0$, $\beta = \frac{-3\alpha^2\sigma_0^2+16c^2-8\alpha c\sigma_0}{\alpha}$. Thus, we get the following

The solitary wave solution:

$$V_{3,6}(x,t) = e^{\gamma\kappa(t)-\frac{\gamma^2}{2}t}\left(\log\left(\frac{2c\coth^2(ct-x)}{\alpha}+\sigma_0\right)\right). \tag{3.36}$$

The dark soliton solution:

$$V_{3,7}(x,t) = e^{\gamma\kappa(t)-\frac{\gamma^2}{2}t}\left(\log\left(\frac{2c\tanh^2(ct-x)}{\alpha}+\sigma_0\right)\right). \tag{3.37}$$

The combo soliton solution:

$$V_{3,8}(x,t) = e^{\gamma\kappa(t)-\frac{\gamma^2}{2}t}\left(\log\left(\frac{2c\tanh^2(ct-x)\left(\coth^4(ct-x)+1\right)}{\alpha}+\sigma_0\right)\right). \tag{3.38}$$

• $\hbar_0 \to \frac{1}{2}$, $\hbar_1 \to 0$, $\hbar_2 \to \frac{1}{2}$ gives $\sigma_1 = 0$, $\sigma_2 = 0$, $\nu_2 = \frac{c}{2\alpha}$, $\eta = \frac{\sigma_0(2\alpha\sigma_0-c)^2}{2\alpha}$, $\nu_1 = 0$, and $\beta = \frac{-12\alpha^2\sigma_0^2-c^2+8\alpha c\sigma_0}{4\alpha}$ along with $\sigma_1 = 0$, $\sigma_2 = \frac{c}{2\alpha}$, $\nu_2 = 0$, $\eta = \frac{\sigma_0(2\alpha\sigma_0-c)^2}{2\alpha}$, $\nu_1 = 0$, $\beta = \frac{-12\alpha^2\sigma_0^2-c^2+8\alpha c\sigma_0}{4\alpha}$, and $\sigma_1 = 0$, $\sigma_2 = \frac{c}{2\alpha}$, $\nu_2 = \frac{c}{2\alpha}$, $\eta = \frac{2(\alpha\sigma_0-c)^2(\alpha\sigma_0+c)}{\alpha^2}$, $\nu_1 = 0$, $\beta = \frac{-3\alpha^2\sigma_0^2+c^2+2\alpha c\sigma_0}{\alpha}$. Therefore, the periodic solutions are as follows:

$$V_{3,9}(x,t) = e^{\gamma\kappa(t)-\frac{\gamma^2}{2}t}\left(\log\left(\frac{c}{2\alpha(\sec(ct-x)-\tan(ct-x))^2}+\sigma_0\right)\right), \tag{3.39}$$

$$V_{3,10}(x,t) = e^{\gamma\kappa(t)-\frac{\gamma^2}{2}t}\left(\log\left(\frac{c(\cot(ct-x)-\csc(ct-x))^2}{2\alpha}+\sigma_0\right)\right), \tag{3.40}$$

$$V_{3,11}(x,t) = e^{\gamma\kappa(t)-\frac{\gamma^2}{2}t}\left(\log\left(\frac{c(\sec(ct-x)-\tan(ct-x))^2}{2\alpha}+\frac{c}{2\alpha(\sec(ct-x)-\tan(ct-x))^2}+\sigma_0\right)\right). \tag{3.41}$$

• For $\hbar_0 \to -\frac{1}{2}$, $\hbar_1 \to 0$, $\hbar_2 \to -\frac{1}{2}$, gives $\sigma_1 = 0$, $\sigma_2 = 0$, $\nu_2 = \frac{c}{2\alpha}$, $\eta = \frac{\sigma_0(2\alpha\sigma_0 - c)2}{2\alpha}$, $\nu_1 = 0$, $\beta = \frac{-12\alpha^2\sigma_0^2 - c^2 + 8\alpha c\sigma_0}{4\alpha}$, along with $\sigma_1 = 0$, $\sigma_2 = \frac{c}{2\alpha}$, $\nu_2 = 0$, $\eta = \frac{\sigma_0(2\alpha\sigma_0 - c)^2}{2\alpha}$, $\nu_1 = 0$, $\beta = \frac{-12\alpha^2\sigma_0^2 - c^2 + 8\alpha c\sigma_0}{4\alpha}$, and $\sigma_1 = 0$, $\sigma_2 = \frac{c}{2\alpha}$, $\nu_2 = \frac{c}{2\alpha}$, $\eta = \frac{2(\alpha\sigma_0 - c)^2(\alpha\sigma_0 + c)}{\alpha^2}$, $\nu_1 = 0$, $\beta = \frac{-3\alpha^2\sigma_0^2 + c^2 + 2\alpha c\sigma_0}{\alpha}$. We then get

$$V_{3,12}(x,t) = e^{\gamma\kappa(t) - \frac{\gamma^2}{2}t}\left(\log\left(\frac{c}{2\alpha(-\cot(ct-x) - \csc(ct-x))^2} + \sigma_0\right)\right), \tag{3.42}$$

$$V_{3,13}(x,t) = e^{\gamma\kappa(t) - \frac{\gamma^2}{2}t}\left(\log\left(\frac{c(\tan(ct-x) + \sec(ct-x))^2}{2\alpha} + \sigma_0\right)\right), \tag{3.43}$$

$$V_{3,14}(x,t) = e^{\gamma\kappa(t) - \frac{\gamma^2}{2}t}\left(\log\left(\frac{c(\tan(ct-x) + \sec(ct-x))^2}{2\alpha} + \frac{c}{2\alpha(\tan(ct-x) + \sec(ct-x))^2} + \sigma_0\right)\right). \tag{3.44}$$

4. Discussion and graphs

In mathematical physics and engineering, two- and three-dimensional graphs are indispensable tools for understanding complex systems inherently influenced by stochastic noise. 2D sketches allow researchers to analyze how noise impacts signal evolution, stability thresholds, and statistical distributions in dynamical systems, signal processing, and quantum mechanics. 3D representations are crucial for capturing the spatial dynamics of noise-affected phenomena, enabling the visualization of stochastic partial differential equation solutions, turbulent fluid flows, electromagnetic field fluctuations, complex optical modes in waveguides, and evolving network topologies under random perturbations. These graphs go beyond idealized models by adding stochastic terms, which show how critical behaviors such as bifurcations, signal degradation, soliton interactions, or resonance phenomena are induced by random fluctuations. Figures 1–8, which represent the respective solutions, have been sketched with the noise effect. Noise affects the propagation of waves by introducing random fluctuations. These fluctuations can disrupt the coherence of the waves, alter signal characteristics, and reduce the amount of information that can be transmitted. In deterministic systems, waves keep their amplitude, phase, and shape constant over time or distance. Stochastic noise, on the other hand, causes random changes that appear as signal degradation. This noise can be thermal, quantum, or environmental. This includes phase jitter, amplitude fading, spectral broadening, and timing errors, and they critically increase bit error rates in optical or radio communications. Noise can trigger wave collapse in nonlinear systems, induce soliton interactions (such as merging or energy exchange), or cause premature decoherence in quantum waves. Conversely, in phenomena like stochastic resonance, carefully tuned noise can paradoxically enhance weak signal detection.

The resulting precise solutions of the extended Zhiber–Shabat-type equation contain a great diversity of wave forms having significant physical explanations. Bright solitons are associated with localized high-amplitude pulses of nonlinear materials, which is the concentration of energy or extreme events. Moreover, in optical communications, bright solitons are physically instantiated as stable light pulses which maintain their shape over transoceanic scales by balancing fiber dispersion with nonlinearity, which forms the basis of high-speed internet infrastructure today. When applied in fluid mechanics, they occur as iconic surface waves such as canal-borne "waves of translation", which

retain coherence due to hydrodynamic nonlinearity and describe the propagation of tsunamis and the dynamics of shallow-water waves. In complex media, bright solitons are the self-trapped packets of waves which fight disorder-scattering with the nonlinear mechanism of self-focusing, enabling the transfer of coherent energy in biological tissues and atmospheric layers. They can be used at the border between mathematics and physics, as they are explicit solutions to integrable systems, offering elusive examples of many-body dynamics that are exactly solvable. Bright soliton concepts are a concept in the new field of data science, which motivates new designs of neural networks with reservoir computing frameworks with models of collisional stability in particles which encode persistent information. They combine and at scales, such as photonic chips to ocean waves, and have mathematical tractability capable of crossing theoretical physics and machine learning uses. Dark solutions are solutions with localized dips on a nonzero background, for example, localized intensity (or phase) defects, or localized propagation of dark pulses. The interaction and coexistence of localized peaks and dips is captured with combined bright dark solutions and are a signature of multicomponent system interactions. Dark solitons in optical communications are more resistant to noise and fiber losses than bright pulses, which make them strong candidates in long-haul transmission of data. They are observed in fluid mechanics as localized depressions of the surface in shallow water holes instead of humps by the nonlinear Schrödinger equation, modeling wave troughs in stratified fluids and oceans, which propagate without change. In complex media, dark solitons are engineered notches in phases that are resistant to those of disordered systems, facilitating the transfer of coherent information by means of biological tissues and turbulent atmospheric pathways in which residual background energy remains. Periodic solutions characterize repeating wave patterns or wave trains that are used in learning more about modulated structures and coherent wave propagation in optical fibers, plasmas and fluids.

In Figure 1, the evolutionary nature shows that an extreme level of noise intensity causes extreme stochastic variability, which results in irregular amplitude variability and a jagged surface profile. Although these perturbations maintain the basic structure of solitons, their evolution is highly unstable, and they lose their smoothness. In Figure 2, with low noise cases, the soliton develops gradually with stable and deterministic curves that stabilize to a constant background amplitude. With a rise in noise intensity, stochastic oscillations begin to form visible jaggedness on the 3D surface and irregular oscillations in the 2D time plots. In the extreme intensity, the solution is highly rough and distorted, but the basic dark soliton dip pattern can still be identified. All in all, noise amplification reduces the smoothness of the solution and adds random variations in amplitude but does not entirely ruin the coherent shape of the soliton. Figure 3 shows the growing intensity of noise results into the more violent initial variations, with the most extreme values increasing notably between approximately 15 and 30. Although the initial development may be chaotic everywhere and with steep spikes, the behavior of the system in the long run changes not to high frequency oscillations but to a swift decay. In the cases of higher intensity, the soliton structure decays upon the first transient again into a flat near-zero state instead of continuing to propagate. This means that the very high noise not only disturbs the soliton, but can also ultimately kill the coherence of it, and the solution can be dissipated. Figure 4 shows that the amplitude dynamic range is increased significantly as noise gets louder; higher peaks and deeper troughs appear. Nevertheless, a central soliton pulse continues to persist, albeit at a higher level of perturbation, which makes it more jagged and displays strikingly sharp step artifacts in the 3D profiles. Temporal evolution exhibits a clear rise-and-fall behavior in which the amplitude of the waves peaks initially before becoming noisy and lower energy. A stronger intensity increases the

maximum amplitude but compromises the smoothness of the solution, forming a highly volatile and jagged wave structure. Moreover, Figure 5 demonstrates that high noise intensity induces significant, random fluctuations in the dark soliton's amplitude and profile. In the 3D plot, the surface appears jagged and rough, indicating that the soliton's depth varies irregularly across space x and time t. The 2D plot confirms this instability, displaying highly oscillatory and noisy trajectories for fixed x values instead of smooth, stable curves. These variations suggest that the noise perturbs the soliton's energy, causing its amplitude to deviate unpredictably from a steady state. Consequently, the coherent structure of the dark soliton is distorted, exhibiting stochastic behavior rather than maintaining a constant depth. In Figures 6 and 7, the real part has large stochastic oscillations and is jagged, which implies that it is highly unstable, and the imaginary part is smooth and has deterministic wave shapes. Although the amplitude of the real component is bigger near 10 with unpredictable behavior, the amplitude of the imaginary component is much lower, close to 0.5, with a coherent structure. Random noise distorts the time evolution of the real part as compared to the predictable and stable pulse propagation of the imaginary part. The 3D plot of the real part is jagged and deformed visually, whereas the imaginary part shows a clear, unperturbed soliton form. In the end, the imaginary part will maintain its soliton integrity, but the real part will be highly degraded by the high level of noise. In Figure 8, the findings imply that with an increase in noise intensity, the soliton evolution process changes to become irregular, with jagged waveforms whose peaks are distorted. At high noise levels, the solution becomes extremely unstable and chaotic, with erratic spikes of large amplitude that works its way through the coherent soliton structure.

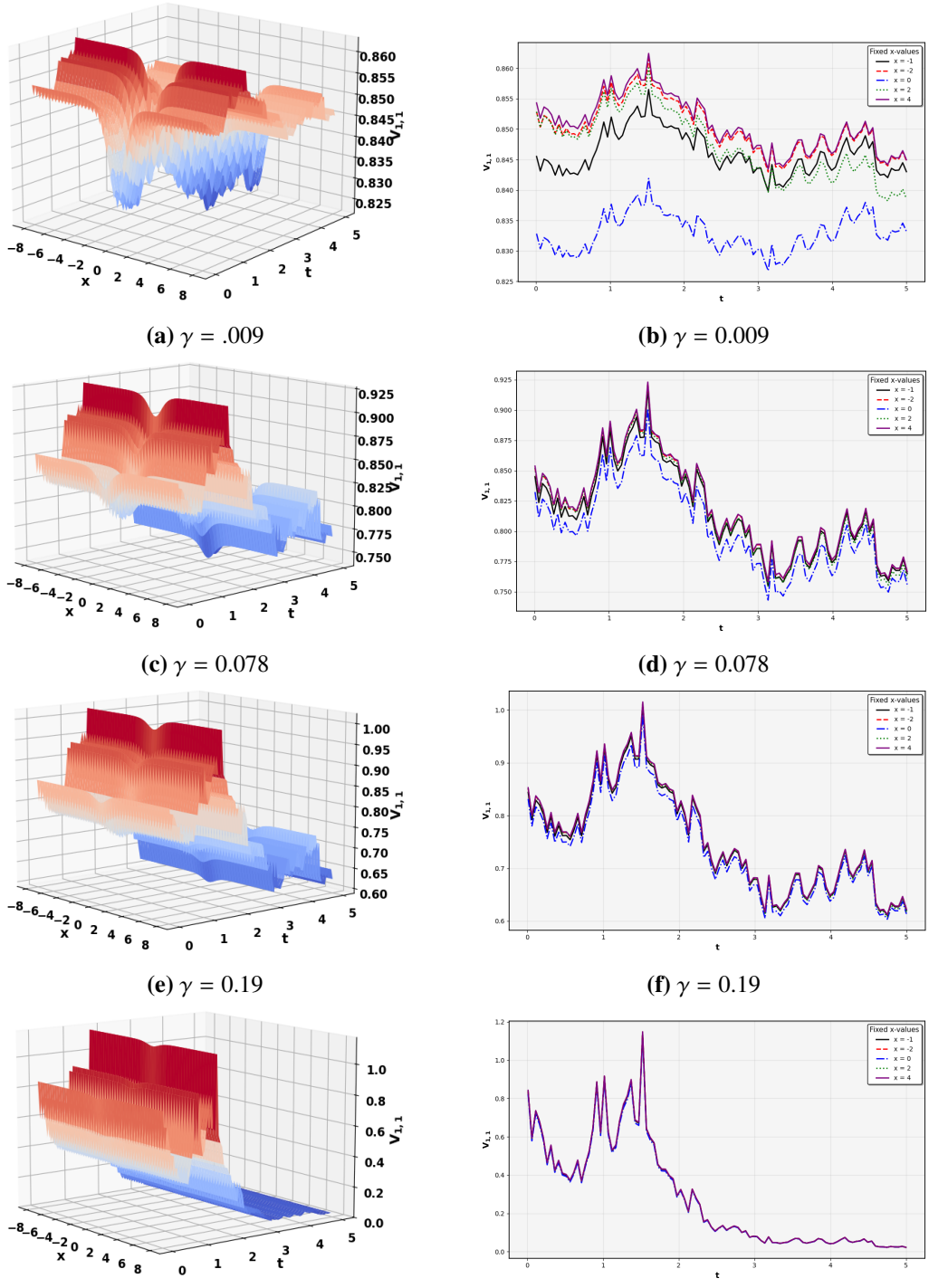

(a) $\gamma = .009$ **(b)** $\gamma = 0.009$

(c) $\gamma = 0.078$ **(d)** $\gamma = 0.078$

(e) $\gamma = 0.19$ **(f)** $\gamma = 0.19$

(g) $\gamma = 0.99$ **(h)** $\gamma = 0.99$

Figure 1. 3D and 2D plots of the solution (3.8) for the parametric values $\alpha = 6.5, \sigma_0 = 2.5, \sigma_2 = .05$.

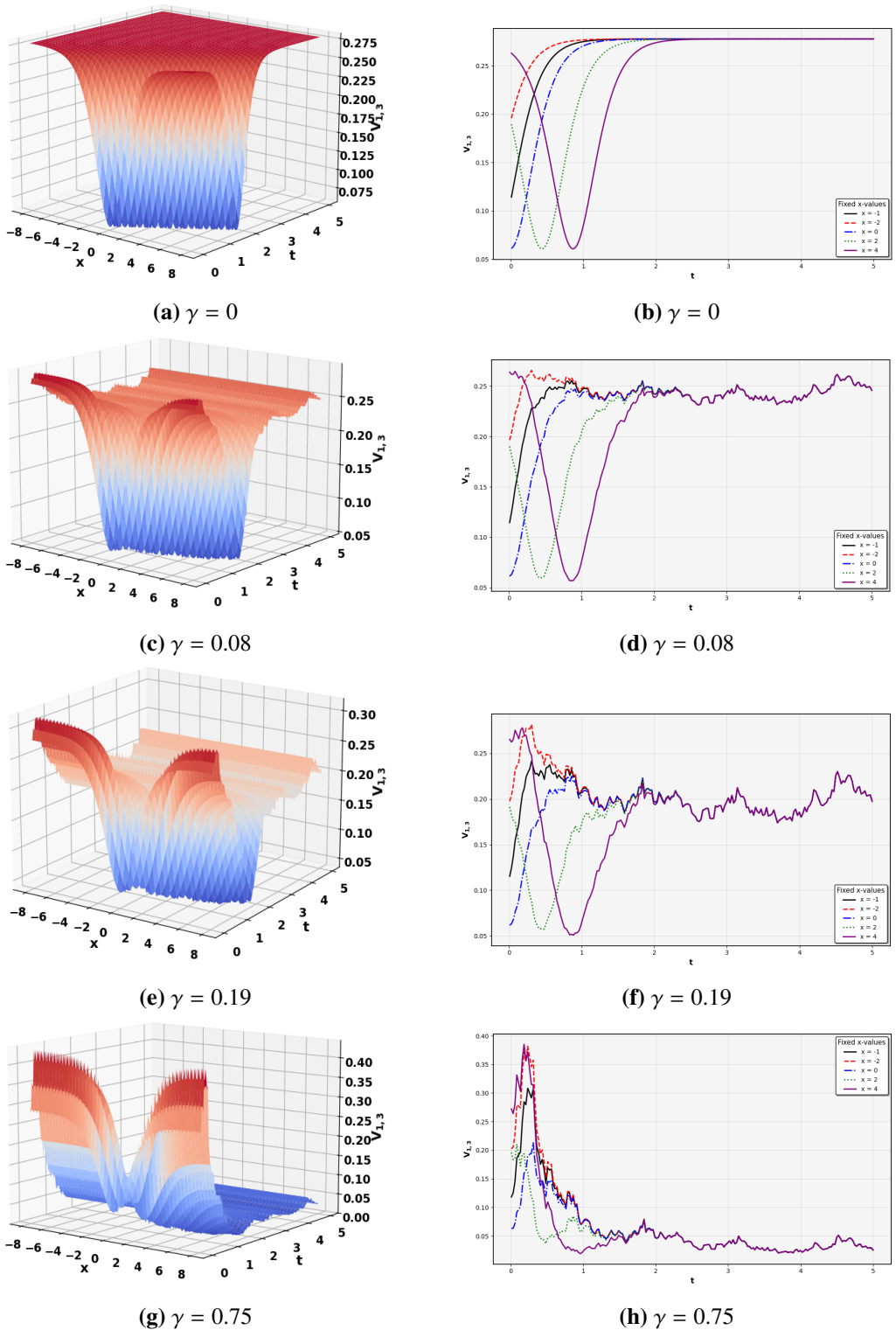

(a) $\gamma = 0$ **(b)** $\gamma = 0$

(c) $\gamma = 0.08$ **(d)** $\gamma = 0.08$

(e) $\gamma = 0.19$ **(f)** $\gamma = 0.19$

(g) $\gamma = 0.75$ **(h)** $\gamma = 0.75$

Figure 2. 3D and 2D plots of the solution (3.10) for the parametric values $\alpha = 9.01, \sigma_0 = 7.5, \sigma_2 = 1.03$.

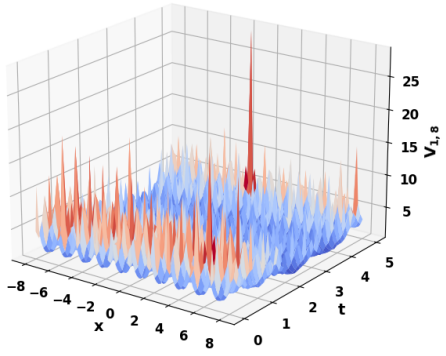

(a) $\gamma = 0.5$

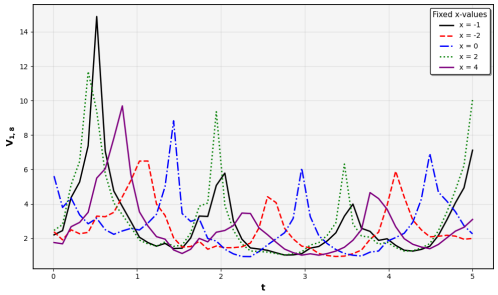

(b) $\gamma = 0.5$

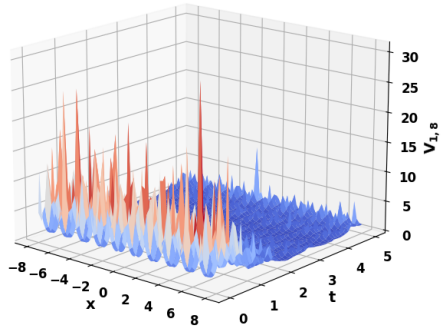

(c) $\gamma = 0.98$

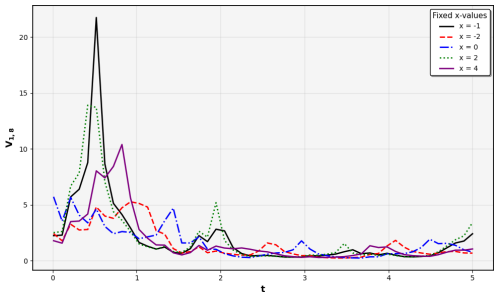

(d) $\gamma = 0.98$

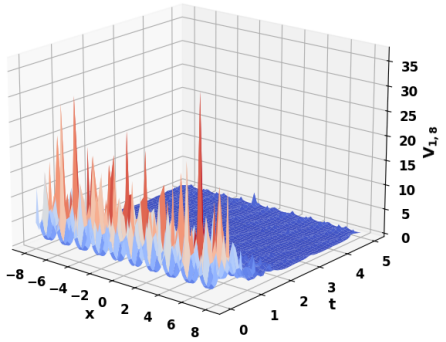

(e) $\gamma = 1.28$

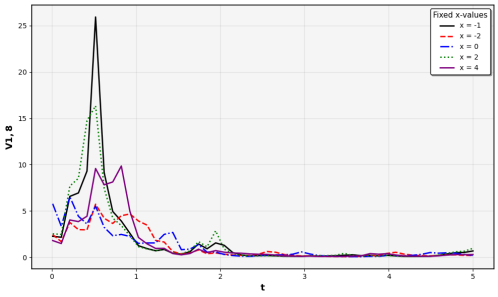

(f) $\gamma = 1.28$

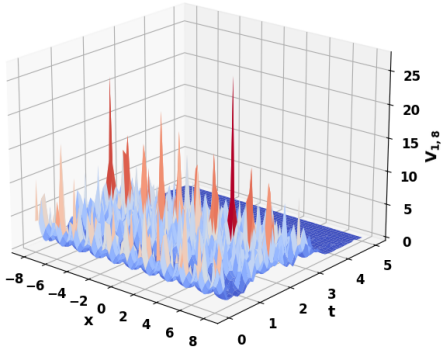

(g) $\gamma = 1.68$

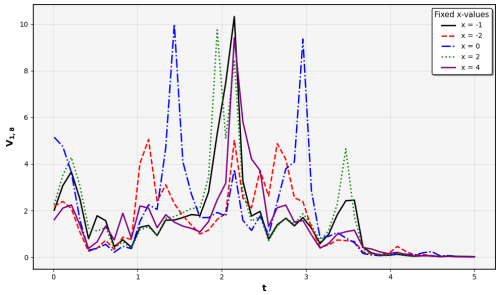

(h) $\gamma = 1.68$

Figure 3. 3D and 2D plots of the solution (3.15) for the parametric values $\sigma_0 = 1.5, \nu_2 = 2.03, \alpha = 1.02$.

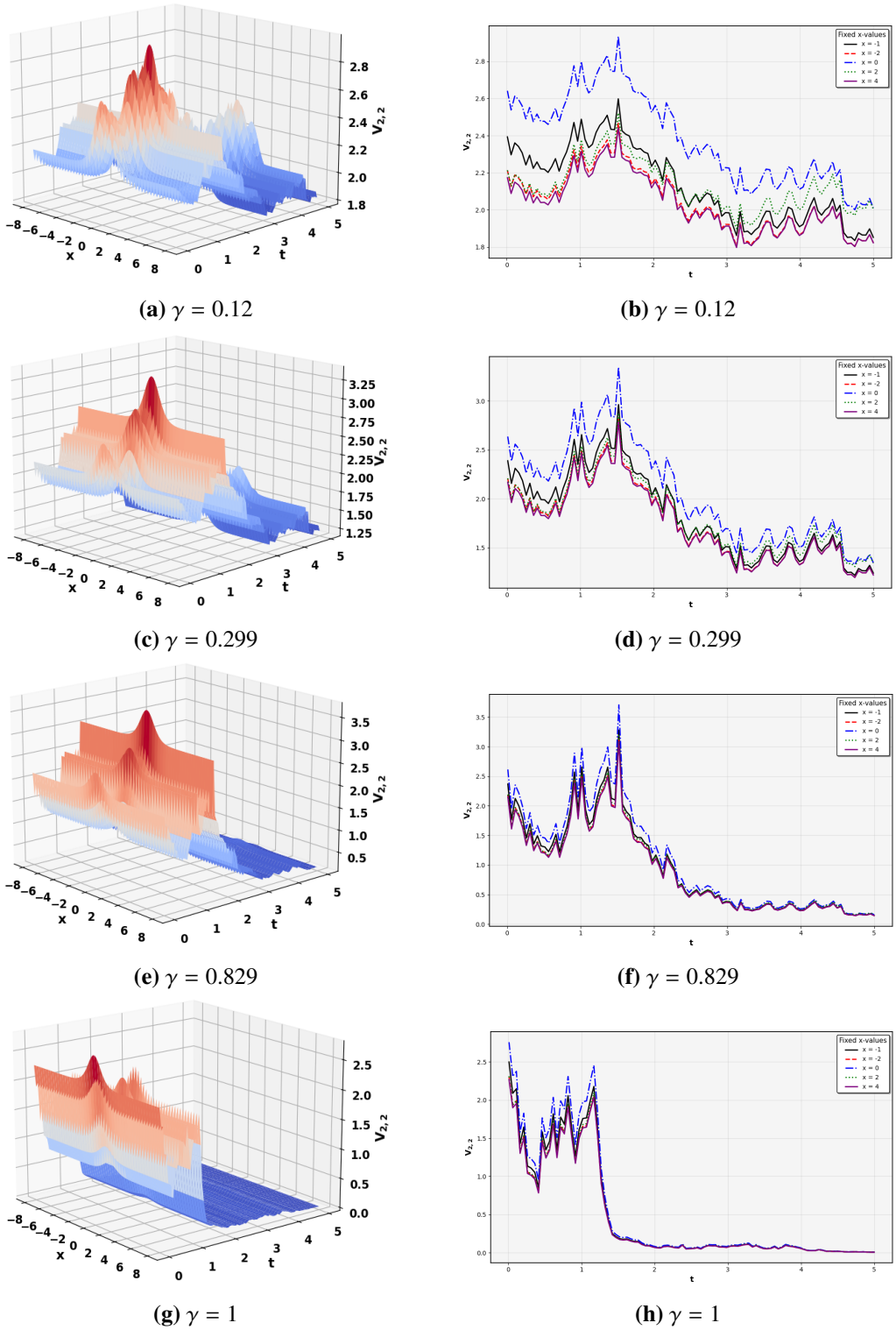

(a) $\gamma = 0.12$ **(b)** $\gamma = 0.12$

(c) $\gamma = 0.299$ **(d)** $\gamma = 0.299$

(e) $\gamma = 0.829$ **(f)** $\gamma = 0.829$

(g) $\gamma = 1$ **(h)** $\gamma = 1$

Figure 4. 3D and 2D plots of the solution (3.24) for the parametric values $\sigma_0 = 6.5, \sigma_2 = 1.2, \nu_2 = 2.3, c = 0.2, A = 0.199$.

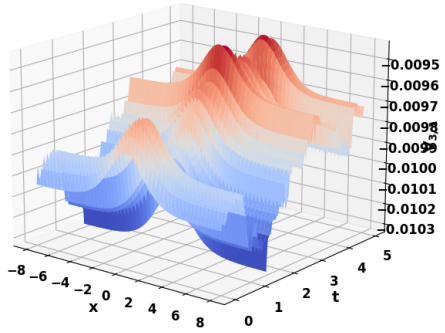

(a) $\gamma = 0.026$

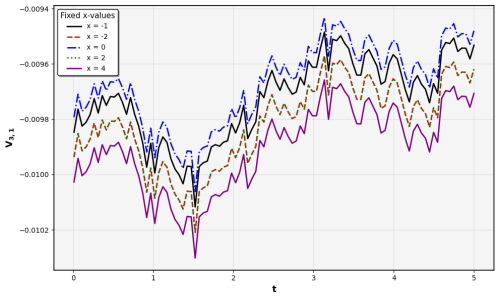

(b) $\gamma = 0.026$

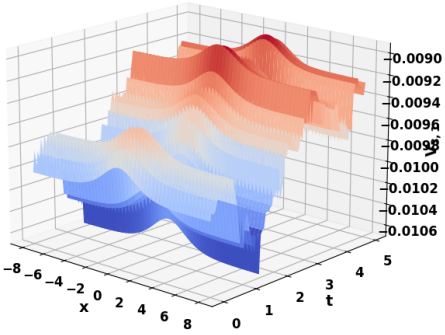

(c) $\gamma = 0.06$

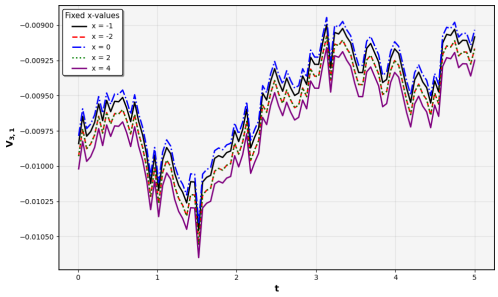

(d) $\gamma = 0.06$

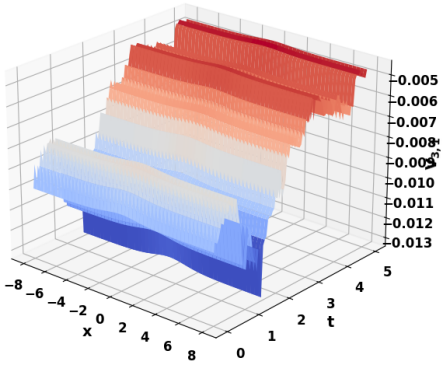

(e) $\gamma = 0.36$

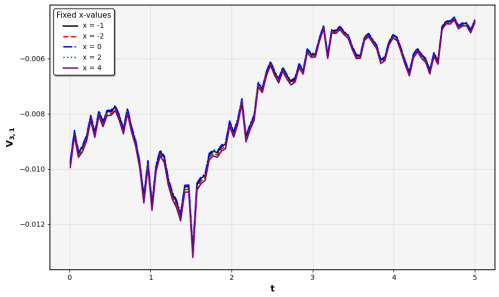

(f) $\gamma = 0.36$

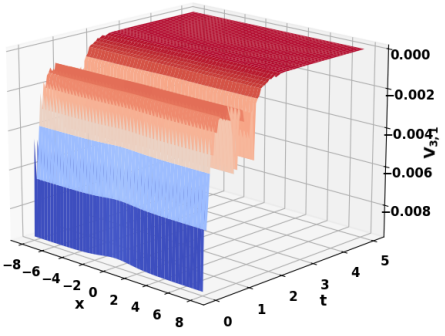

(g) $\gamma = 1.996$

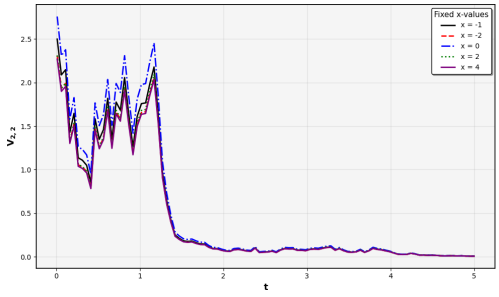

(h) $\gamma = 1.996$

Figure 5. 3D and 2D plots of the solution (3.31) for the parametric values $\sigma_0 = 0.99, \sigma_1 = 0.001, \eta = 0.56$.

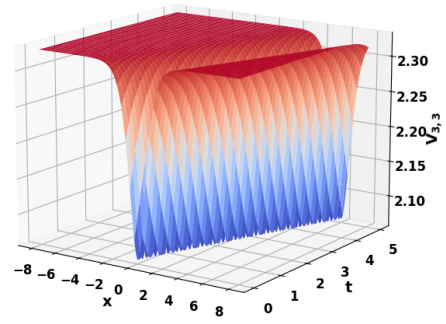

(a) $\gamma = 0$

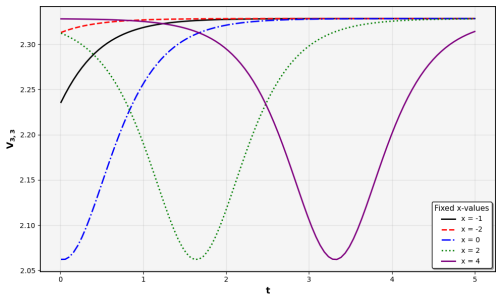

(b) $\gamma = 0$

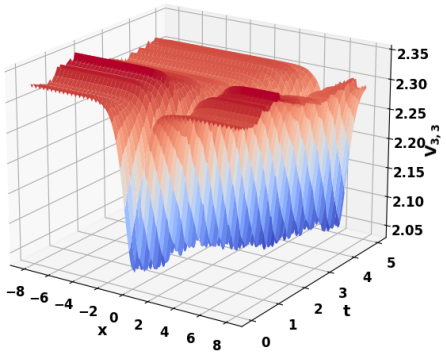

(c) $\gamma = 0.009$

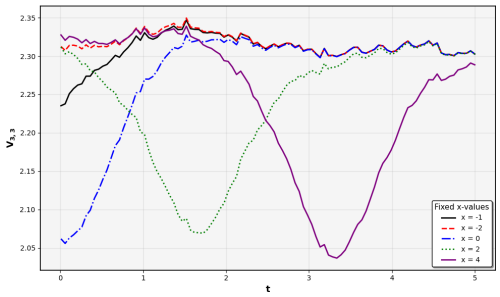

(d) $\gamma = 0.009$

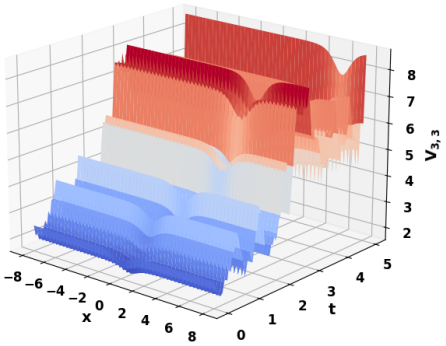

(e) $\gamma = 0.6$

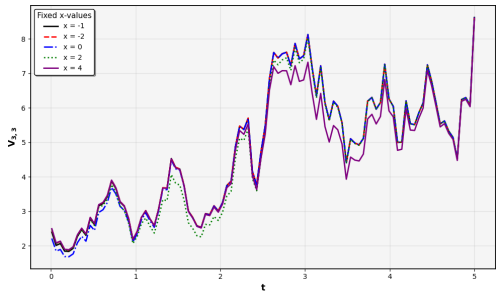

(f) $\gamma = 0.6$

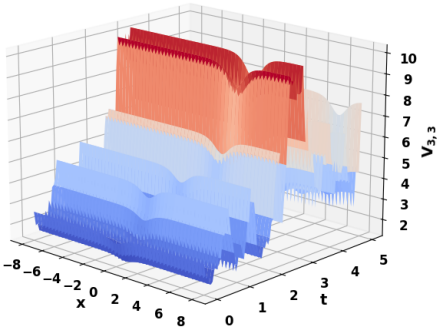

(g) $\gamma = 0.996$

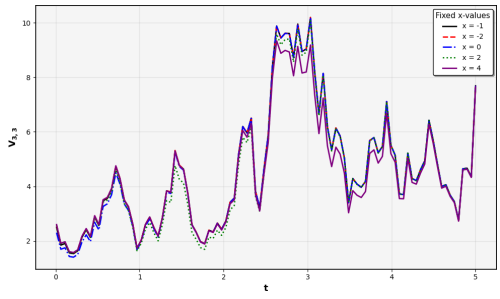

(h) $\gamma = 0.996$

Figure 6. 3D and 2D plots of the real part of the solution (3.33) for the parametric values $\sigma_0 = 9.06, c = 1.2, \alpha = 0.5$.

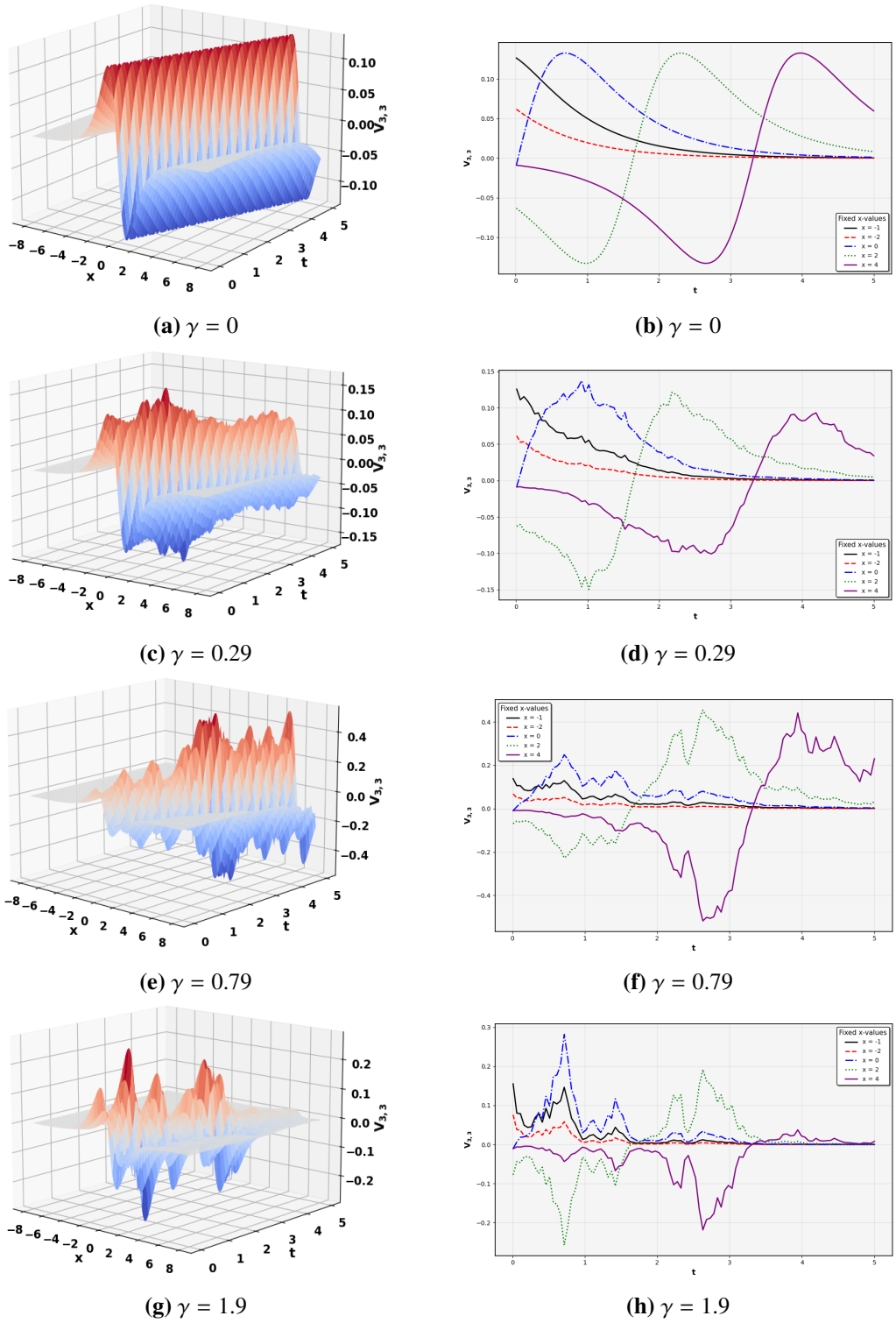

(a) $\gamma = 0$ **(b)** $\gamma = 0$

(c) $\gamma = 0.29$ **(d)** $\gamma = 0.29$

(e) $\gamma = 0.79$ **(f)** $\gamma = 0.79$

(g) $\gamma = 1.9$ **(h)** $\gamma = 1.9$

Figure 7. 3D and 2D plots of the imaginary part of the solution (3.33) for the parametric values $\sigma_0 = 9.06, c = 1.2, \alpha = 0.5$.

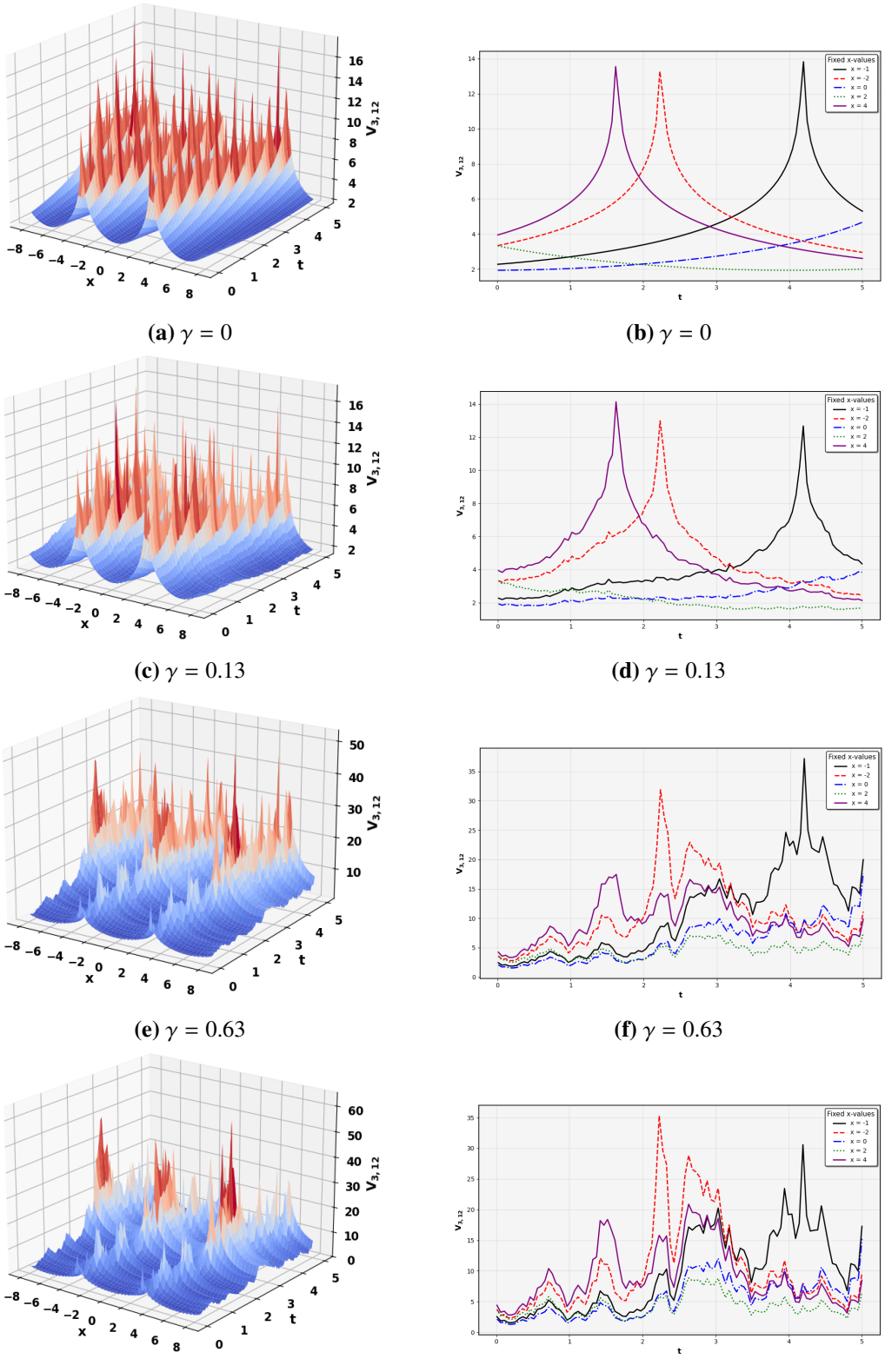

(a) $\gamma = 0$ **(b)** $\gamma = 0$

(c) $\gamma = 0.13$ **(d)** $\gamma = 0.13$

(e) $\gamma = 0.63$ **(f)** $\gamma = 0.63$

(g) $\gamma = 1$ **(h)** $\gamma = 1$

Figure 8. 3D and 2D plots of the imaginary part of the solution (3.42) for the parametric values $\sigma_0 = 6.9, c = 0.5, \alpha = 0.03$.

5. Conclusions

In this work, we examined the nonlinear dynamical behaviors of stochastic Zhiber-Shabat model with the application of newly developed techniques, including the F-expansion approach, mGERFM, and the modified Arnous method with Wolfram Mathematica 13.3. This work has effectively developed a diverse array of solutions, including dark, periodic, bright, singular, hyperbolic, and exponential soliton solutions. Consequently, it provides a wide range of information about the system's properties. The results demonstrate the efficacy of the proposed methods in enhancing soliton theory and its importance in generating solitary waves for various nonlinear complicated systems. Visual representations have been added to illustrate the findings behaviors by the assistance of computer language Python 3.13.0 with https: $//www.python.org/downloads/release/python-3130/$. The obtained solutions are pertinent to several disciplines, including engineering, applied sciences, mathematical physics, and nonlinear dynamics. These results can pique the curiosity of researchers looking at frameworks for nonlinear problems in the applied sciences. In future work, the stochastic Zhiber–Shabat model can be extended to include additional physical effects such as variable coefficients or higher-order nonlinear terms to better describe complex wave phenomena. Furthermore, stability analysis and numerical simulations may be conducted to investigate the long-time behavior and physical implications of the obtained stochastic wave solutions. The findings are intriguing from both a practical and theoretical perspective, particularly when considering the behavior of numerous nonlinear models with the addition of stochastic terms.

Author contributions

Jan Muhammad: Methodology, software, validation, formal analysis; Ali H. Tedjani: Resources, funding acquisition, project administration; Usman Younas: Writing–review & editing, supervision, visualization. All authors have read and approved the final version of the manuscript for publication.

Use of Generative-AI tools declaration

The authors declare they have not used artificial intelligence (AI) tools in the creation of this article.

Funding

This work was supported and funded by the Deanship of Scientific Research at Imam Mohammad Ibn Saud Islamic University (IMSIU) (Grant No. IMSIU-DDRSP2602).

Conflict of interest

The authors declare no conflicts of interest.

References

1. R. E. Ecke, Chaos, patterns, coherent structures, and turbulence: reflections on nonlinear science, *Chaos*, **25** (2015), 097605. https://doi.org/10.1063/1.4915623

2. M. J. Feigenbaum, Universal behavior in nonlinear systems, *Physica D*, **7** (1983), 16–39. https://doi.org/10.1016/0167-2789(83)90112-4

3. A. Başhan, Y. Uçar, N. M. Yağmurlu, A. Esen, Numerical solution of the complex modified Korteweg-de Vries equation by DQM, *J. Phys.: Conf. Ser.*, **766** (2016), 012028. https://doi.org/10.1088/1742-6596/766/1/012028

4. G. Nicolis, *Introduction to nonlinear science*, Cambridge: Cambridge University Press, 1995. https://doi.org/10.1017/CBO9781139170802

5. A. Başhan, Modification of quintic B-spline differential quadrature method to nonlinear Korteweg-de Vries equation and numerical experiments, *Appl. Numer. Math.*, **167** (2021), 356–374. https://doi.org/10.1016/j.apnum.2021.05.015

6. L. Ming, J. Muhammad, D. Yaro, U. Younas, Exploring the multistability, sensitivity, and wave profiles to the fractional Sharma–Tasso–Olver equation in the mathematical physics, *AIP Adv.*, **15** (2025), 045017. https://doi.org/10.1063/5.0264311

7. J. L. Shen, J. Muhammad, U. Younas, Investigating the wave dynamics and interaction structures: Exploring the Benney-Roskes/Zakharov-Rubenchik model in the oceanic atmosphere, *Ocean Eng.*, **354** (2026), 124969. https://doi.org/10.1016/j.oceaneng.2026.124969

8. J. Muhammad, M. Bilal, S. Ur Rehman, N. Nasreen, U. Younas, Analyzing the decoupled nonlinear Schrödinger equation: fractional optical wave patterns in the dual-core fibers, *J. Opt.*, **2024** (2024), 1–12. https://doi.org/10.1007/s12596-024-02236-8

9. A. Başhan, A. Esen, Single soliton and double soliton solutions of the quadratic-nonlinear Korteweg-de Vries equation for small and long-times, *Numer. Meth. Part. D. E.*, **37** (2021), 1561–1582. https://doi.org/10.1002/num.22597

10. D. L. Wang, Z. X. Liu, H. P. Zhao, H. Q. Qin, G. X. Bai, C. Chen, et al., Launching by cavitation, *Science*, **389** (2025), 935–939. https://doi.org/10.1126/science.adu8943

11. D. S. Mou, Z. Z. Si, W. X. Qiu, C. Q. Dai, Optical soliton formation and dynamic characteristics in photonic Moiré lattices, *Opt. Laser Technol.*, **181** (2025), 111774. https://doi.org/10.1016/j.optlastec.2024.111774

12. A. Başhan, An effective approximation to the dispersive soliton solutions of the coupled KdV equation via combination of two efficient methods, *Comp. Appl. Math.*, **39** (2020), 80. https://doi.org/10.1007/s40314-020-1109-9

13. A. Başhan, N. M. Yağmurlu, Y. Uçar, A. Esen, A new perspective for the numerical solution of the modified equal width wave equation, *Math. Method. Appl. Sci.*, **44** (2021), 8925–8939. https://doi.org/10.1002/mma.7322

14. A. H. Arnous, Optical solitons with Biswas–Milovic equation in magneto-optic waveguide having Kudryashov's law of refractive index, *Optik*, **247** (2021), 167987. https://doi.org/10.1016/j.ijleo.2021.167987

15. B. Kopcasiz, F. N. K. Sağlam, S. Malik, Exact soliton solutions for the (n+1)-dimensional generalized Kadomtsev–Petviashvili equation via two novel methods, *Int. J. Geom. Methods M.*, **22** (2025), 2550105. https://doi.org/10.1142/S0219887825501051

16. F. N. K. Sağlam, B. Kopçasız, M. Şenol, Abundant new soliton solutions to the Arshed–Biswas equation via two novel integrating schemes, *Mod. Phys. Lett. A*, **40** (2025), 2550054. https://doi.org/10.1142/S0217732325500543

17. F. N. K. Sağlam, Analytical approaches to the stochastic nonlinear Kodama equation via the impact of multiplicative noise, *Math. Method. Appl. Sci.*, **48** (2025), 15092–15110. https://doi.org/10.1002/mma.70002

18. S. Z. Majid, M. I. Asjad, W. A. Faridi, Formation of solitary waves solutions and dynamic visualization of the nonlinear schrödinger equation with efficient techniques, *Phys. Scr.*, **99** (2024), 065255. https://doi.org/10.1088/1402-4896/ad4b10

19. U. Younas, J. Muhammad, Q. Ali, M. Sediqmal, K. Kedzia, A. Z. Jan, On the study of solitary wave dynamics and interaction phenomena in the ultrasound imaging modelled by the fractional nonlinear system, *Sci. Rep.*, **14** (2024), 26080. https://doi.org/10.1038/s41598-024-75494-y

20. E. Yaşar, Y. Yıldırım, C. M. Khalique, Lie symmetry analysis, conservation laws and exact solutions of the seventh-order time fractional Sawada–Kotera–Ito equation, *Results Phys.*, **6** (2016), 322–328. https://doi.org/10.1016/j.rinp.2016.06.003

21. H. H. Hussein, K. K. Ahmed, H. M. Ahmed, A. Elsheikh, W. Alexan, Existence of novel analytical soliton solutions in a magneto-electro-elastic annular bar for the longitudinal wave equation, *Opt. Quant. Electron.*, **56** (2024), 1344. https://doi.org/10.1007/s11082-024-07218-5

22. H. H. Hussein, H. M. Ahmed, W. B. Rabie, K. K. Ahmed, M. S. Hashemi, M. Bayram, Multiple soliton solutions and other travelling wave solutions to new structured (2+1)-dimensional integro-partial differential equation using efficient technique, *Phys. Scr.*, **99** (2024), 105270. https://doi.org/10.1088/1402-4896/ad7993

23. I. Samir, H. M. Ahmed, H. Emadifar, K. K. Ahmed, Traveling and soliton waves and their characteristics in the extended (3+1)-dimensional Kadomtsev–Petviashvili equation in fluid, Partial *Partial Differential Equations in Applied Mathematics*, **14** (2025), 101146. https://doi.org/10.1016/j.padiff.2025.101146

24. A. R. Seadawy, A. Ali, T. Radwan, W. W. Mohammed, K. K. Ahmed, Solitary wave solutions for the conformable time-fractional coupled Konno-Oono model via applications of three mathematical methods, *AIMS Mathematics*, **10** (2025), 16027–16044. https://doi.org/10.3934/math.2025718

25. M. H. Ali, H. M. Ahmed, A. Abd-Elmonem, N. A. A. Suoliman, K. K. Ahmed, I. Samir, Optical solitons for generalised perturbed nonlinear Schrödinger model in the presence of dual-power law nonlinear medium, *Optik*, **319** (2024), 172112. https://doi.org/10.1016/j.ijleo.2024.172112

26. M. E. Ramadan, H. M. Ahmed, A. S. Khalifa, K. K. Ahmed, Analytical study of fractional solitons in three dimensional nonlinear evolution equation within fluid environments, *Sci. Rep.*, **15** (2025), 35399. https://doi.org/10.1038/s41598-025-12576-5

27. J. W. Li, J. C. Shi, X. Y. Pang, M. R. Belić, D. Mihalache, W. Q. Qin, et al., Spontaneous symmetry and antisymmetry breaking of solitons in quintic nonlinearity, *Chaos Soliton. Fract.*, **202** (2026), 117562. https://doi.org/10.1016/j.chaos.2025.117562

28. L. W. Zeng, J. S. He, B. A. Malomed, J. B. Chen, X. Zhu, Spontaneous symmetry and antisymmetry breaking of two-component solitons in a combination of linear and nonlinear double-well potentials, *Phys. Rev. E*, **110** (2024), 064216. https://doi.org/10.1103/PhysRevE.110.064216
29. X. Zhu, M. R. Belić, D. Mihalache, J. W. Li, L. W. Zeng, Dark solitons in purely quintic nonlinear lattices with defects, *Chaos Soliton. Fract.*, **200** (2025), 116983. https://doi.org/10.1016/j.chaos.2025.116983
30. X. Zhu, Y. Fan, M. R. Belić, D. Mihalache, D. Xiang, L. W. Zeng, Optical dark solitons in purely cubic-quintic nonlinear lattices, *Opt. Express*, **33** (2025), 7205–7217. https://doi.org/10.1364/OE.553947
31. Y. H. Jia, Z. Z. Si, Z. T. Ju, H. Y. Feng, J. H. Zhang, X. Yan, et al., Convolutional-recurrent neural network for the prediction of formation and switching dynamics for multicolor solitons, *Sci. China Phys. Mech. Astron.*, **68** (2025), 284211. https://doi.org/10.1007/s11433-025-2679-8
32. Z. Z. Si, D. L. Wang, B. W. Zhu, Z. T. Ju, X. P. Wang, W. Liu, et al., Deep learning for dynamic modeling and coded information storage of vector-soliton pulsations in mode-locked fiber lasers, *Laser Photonics Rev.*, **18** (2024), 2400097. https://doi.org/10.1002/lpor.202400097
33. Z. Z. Si, Z. T. Ju, L. F. Ren, X. P. Wang, B. A. Malomed, C. Q. Dai, Polarization-induced buildup and switching mechanisms for soliton molecules composed of noise-like-pulse transition states, *Laser Photonics Rev.*, textbf19 (2025), 2401019. https://doi.org/10.1002/lpor.202401019
34. H. K. Hu, Distributed constrained optimization for nonlinear stochastic multi-agent systems: application to resource allocation, *Complex Systems Stability and Control*, **1** (2025), 5. https://doi.org/10.53941/cssc.2025.100005
35. H. Q. Peng, Q. X. Zhu, Finite-time stability and stabilization of highly nonlinear stochastic systems via the noise control, *IEEE T. Automat. Contr.*, **99** (2026), 1–8. https://doi.org/10.1109/TAC.2026.3660601
36. Q. X. Zhu, Event-triggered sampling problem for exponential stability of stochastic nonlinear delay systems driven by Lévy processes, *IEEE T. Automat. Contr.*, **70** (2024) 1176–1183. https://doi.org/10.1109/TAC.2024.3448128
37. S. Ur Rehman, J. Ahmad, T. Muhammad, Dynamics of novel exact soliton solutions to stochastic Chiral nonlinear Schrodinger equation, *Alex. Eng. J.*, **79** (2023), 568–580. https://doi.org/10.1016/j.aej.2023.08.014
38. A. H. Arnous, Optical solitons to the cubic quartic Bragg gratings with anti-cubic nonlinearity using new approach, *Optik*, **251** (2022), 168356. https://doi.org/10.1016/j.ijleo.2021.168356
39. N. Ozdemir, A. Secer, M. Ozisik, M. Bayram, Optical soliton solutions of the nonlinear Schrödinger equation in the presence of chromatic dispersion with cubic-quintic-septic-nonicnonlinearities, *Phys. Scr.*, **98** (2023), 115223. https://doi.org/10.1088/1402-4896/acff50
40. M. W. Yasin, M. Z. Baber, A. Butt, I. Saeed, T. A. Sulaiman, A. Yusuf, et al., Visualization of the impact of noise of the closed-form solitary wave solutions for the stochastic Zhiber–Shabat model, *Mod. Phys. Lett. A*, **40** (2025), 2550077. https://doi.org/10.1142/S0217732325500774

41. A. M. Wazwaz, The tanh method for travelling wave solutions to the Zhiber–Shabat equation and other related equations, *Commun. Nonlinear Sci.*, **13** (2008), 584–592. https://doi.org/10.1016/j.cnsns.2006.06.014

42. A. Yokus, H. Durur, H. Ahmad, S. W. Yao, Construction of different types analytic solutions for the Zhiber-Shabat equation, *Mathematics*, **8** (2020), 908. https://doi.org/10.3390/math8060908

43. M. Inc, New type soliton solutions for the Zhiber–Shabat and related equations, *Optik*, **138** (2017), 1–7. https://doi.org/10.1016/j.ijleo.2017.02.103

44. A. M. A. Adam, E. A. E. Gumma, A. Satty, M. Salih, Z. M. S. Mohammed, G. S. M. Khamis, et al., Analytical solutions to the fractional Zhiber–Shabat equation using the unified method, *Int. J. Anal. Appl.*, **23** (2025), 230. https://doi.org/10.28924/2291-8639-23-2025-230

45. A. Khalifa, H. Ahmed, K. K. Ahmed, Construction of exact solutions for a higher-order stochastic modified Gerdjikov–Ivanov model using the IMETF method, *Phys. Scr.*, (2024). https://doi.org/10.1088/1402-4896/ada321

46. J. Muhammad, U. Younas, Y. Alrashedi, M. Alhazmi, Analyzing the diversity of wave profiles to the stochastic Davey–Stewartson equation: application in the hydrodynamics engineering, *Ain Shams Eng. J.*, **16** (2025), 103701. https://doi.org/10.1016/j.asej.2025.103701

AIMS Press

© 2026 the Author(s), licensee AIMS Press. This is an open access article distributed under the terms of the Creative Commons Attribution License (https://creativecommons.org/licenses/by/4.0)